Toggle navigation

- **Hello Dr Karsa** (logout)
- Help
- Profile
- Contact

Toggle navigation

- Start
- My Abstracts
- Guidelines

Feedback / Support

×

How can we help you?

How can we improve the system for you?

Please enter your message here.

Close Send feedback

-
- Attributes
- Authors
- Topic
- Content
- Questions
- Preview
- Submission

«

»

Preview

Summary

Topic:
MRI Development and Validation: Image Analysis and Post-Processing
Type:
Oral Presentation
Abstract no.:
A-1104
Status:
complete (not submitted)
Young Investigator Award - Boost your Career! (and win € 1,000) :
No, I won't apply for the Young Investigator Award
Moderator at ESMRMB 2020 Congress:
No, I will not apply to become a moderator

Simultaneous Noise Suppression and Edge Preservation in MRI Conductivity Mapping

A. Karsa, K. Shmueli

- University College London, Medical Physics and Biomedical Engineering, London, United Kingdom

Introduction

Conductivity Mapping (CM) is a new quantitative, non-invasive technique that could provide new information on tissue ion content, specifically on sodium levels[1], and distinguish between brain tumour types[2].

The electrical conductivity (σ) is a complicated function of the MRI phase at TE = 0 ms (φ_0) but the following **differential** equation is a widely-used approximation, valid in regions with slowly varying σ:
$\sigma = (\mu_0\omega)^{-1} \cdot \nabla^2\varphi_0$ [1]
μ_0 = vacuum permeability, ω = Larmor angular frequency, and ∇^2 = Laplacian operator. Calculating ∇^2 using a small kernel (Fig. 2a) tends to severly amplify the noise (Fig. 3a), while larger kernels[3] (Fig. 2b) induce inaccuracies and blurring near the tissue boundaries with σ jumps (Fig. 3b).
It has been suggested that the **integral** form[4] of Eq. 1 is more robust to noise[5]:
$\sigma = (\mu_0\omega V)^{-1} \cdot \int_S \nabla\varphi_0 \, d\boldsymbol{s}$ [2]
S is the closed surface of some kernel with volume V. Again, larger V are expected to suppress noise but cause blurring.

Previous studies have used i) Eq. 1 with large kernels combined with either magnitude-based weighting[6] (*Mag*) or image segmentation[3] (*Seg*) to provide better edge preservation, or ii) Eq. 2 only with small kernels to avoid errors at the tissue boundaries[4-5].

Here we implemented Eq. 2 using large kernels restricted by the magnitude (*Mag*) and/or the segmentation (*Seg*). We compared several differential- and integral-based approaches in a numerical phantom and an in-vivo brain image.

Subjects/Methods

A numerical brain phantom (Fig. 1a) with realistic conductivity and magnitude values was created from the Zubal phantom[7]. φ_0 was simulated using ∇^{-2} (the inverse of Eq. 1) and Gaussian noise (standard deviation = 0.05) was added to the real and imaginary parts.

Multi-echo brain images were acquired in a healthy volunteer at 3T (Fig. 1b). ASPIRE[8] was used on the first

two echoes to estimate φ_0 for each channel which were then combined using scalar phase matching[9]. The gray and white matter, and cerebrospinal fluid were segmentated using SPM12[10] on the combined magnitude image.

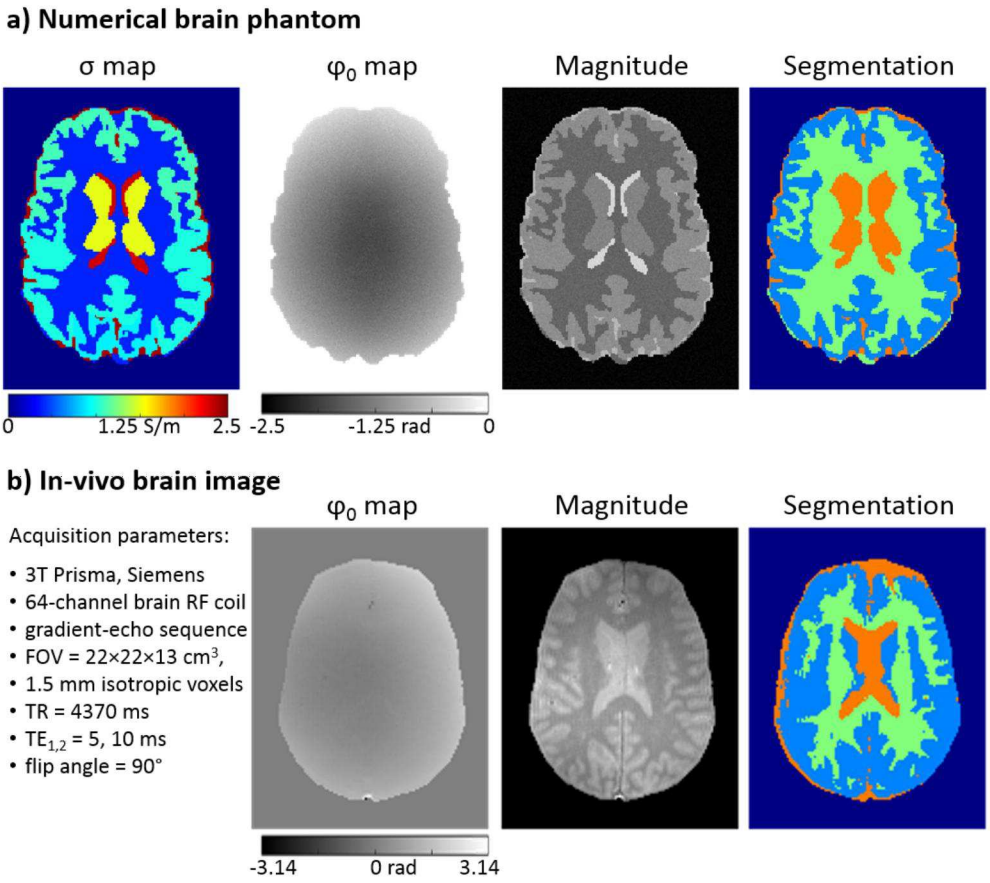

Fig. 1: The numerical brain phantom (a) and the in-vivo brain image (b) including the acquisition parameters.

σ maps were calculated from both the in-vivo and simulated φ_0 using both Eq. 1 and 2 with (Fig 2.): a) small kernels, b) large kernels, c) *Mag*, d) *Seg*, and e) *Mag+Seg*.

	a) Small kernel	b) Larger kernel	c) Mag	d) Seg	e) Mag+Seg
Differential-based (Eq. 1) approaches	∇^2 is calculated using the finite difference approximation. Kernel: 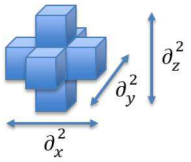	∇^2 is calculated by fitting a 3D quadratic function to all voxels within a 10 mm radius.	The quadratic fit from b) is weighted by the magnitude[6] (i.e. voxels with similar magnitudes to the middle voxel get higher weights).	The quadratic fit from b) is performed within each segment separately.	c) and d) combined. The quadratic fit from b) is performed within each segment separately with magnitude weighting[6].
			The kernel radius is 12 and 15 mm for the phantom and in-vivo image respectively.		
Integral-based (Eq. 2) approaches	1. ∇ is calculated using the finite difference approximation. Kernel: 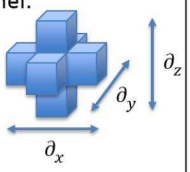	1. ∇ is calculated by fitting a 3D quadratic function to all voxels within a 6 mm radius.	1. The quadratic fit from b) is weighted by the magnitude[6]	1. The quadratic fit from b) is performed within each segment separately.	1. c) and d) combined. The quadratic fit from b) is performed within each segment separately with magnitude weighting[6].
			The kernel radius is 8 and 10.5 mm for the phantom and in-vivo image respectively.		
	2. The surface integral is performed for kernel (V): 	2. The surface integral is performed for a sphere of radius = 6 mm.	2. Voxels with substantially different magnitudes (more than 3*std(Magnitude) away) from the middle voxel are excluded from the kernel (V) before the surface integral is performed.	2. Voxels of different segments from the middle voxel are excluded from the kernel (V) before the surface integral is performed.	2. c) and d) combined. Both voxels with substantially different magnitudes and different segments are excluded from the kernel (V) before the surface integral is performed.
			The kernel radius is 12 and 15 mm for the phantom and in-vivo image respectively.		

Fig. 2: A detailed description of all conductivity mapping techniques implemented and their parameters optimised for the numerical phantom and in-vivo images used in this study.

Discussion

Fig. 3 shows that compared to b), all σ maps were substantially improved by using either *Mag* (white ellipses) or *Seg* (black ellipses) especially near the edges. *Mag+Seg* yielded further improvements (white arrows). The integral-based approaches always yielded much better edge preservation than the differential-based methods (white rectangles). **To sum up, integral-based CM with *Mag+Seg (Fig 2.)* provided the best σ maps from noisy phase.**

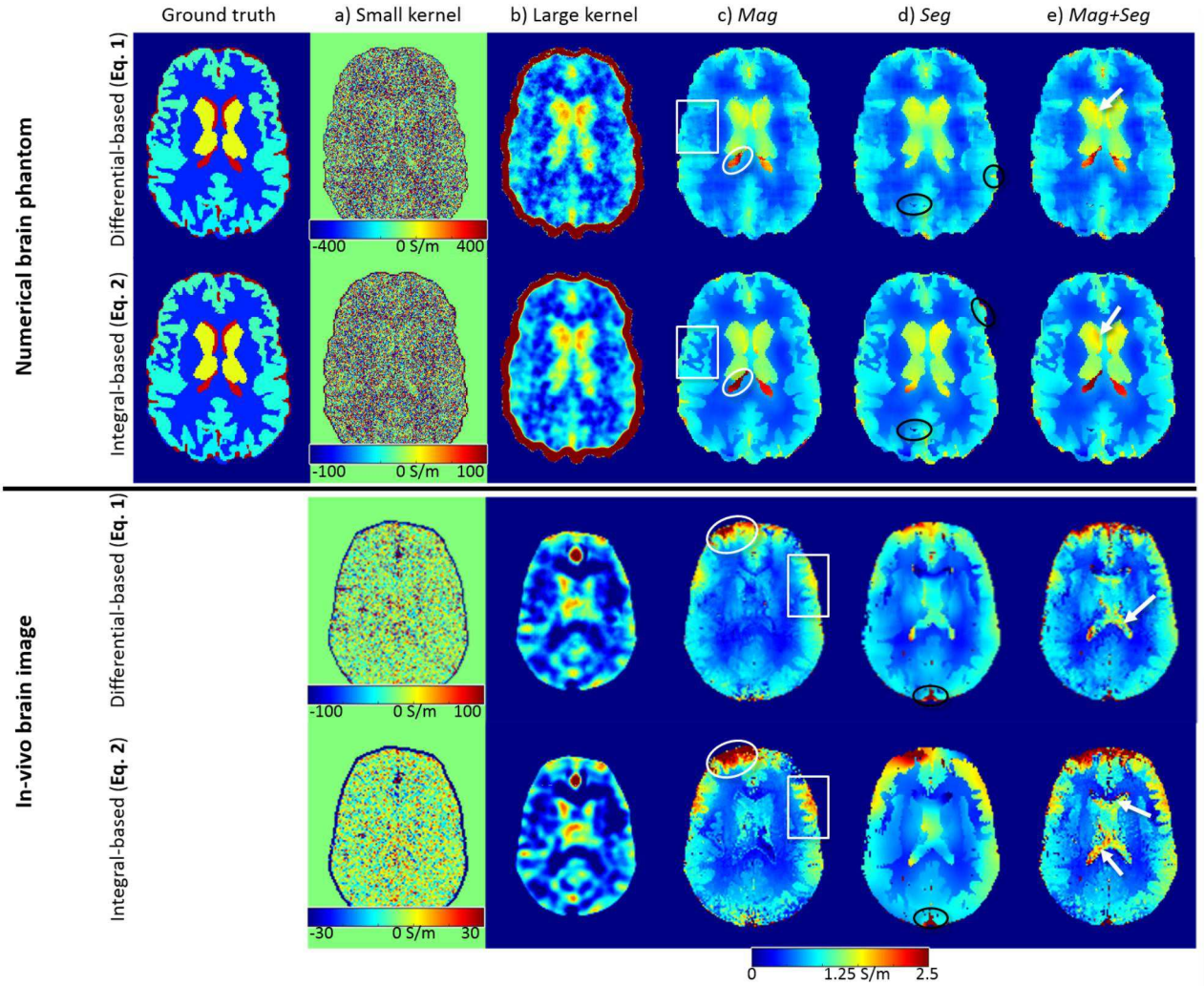

Fig. 3: All σ maps calculated using the methods from Fig. 2. White and black ellipses, and white arrows show regions where Mag, Seg, or Mag+Seg improved the images. The white rectangles highlight the superior performance of the integral-based methods

References

[1]Katscher *NMR in Biomed* 30.8 (2017) [2]Tha *Proc ISMRM* (2016) [3]Katscher *Proc ISMRM* (2012) [4]Voigt *MRM* 66.2 (2011) [5]Bulumulla *Proc ISMRM* (2012) [6]Lee *MRM* 76.2 (2016) [7]Zubal *Med Phys* 21.2 (1994) [8]Eckstein *MRM* 79.6 (2018) [9]Hammond *Neuroim.* 39.4 (2008) [10]fil.ion.ucl.ac.uk/spm/software/spm12

Authors

First author:
Anita Karsa
Presented by:
Anita Karsa
Submitted by:
Anita Karsa

Proceed to abstract submission

Return to last page

Deadline:

2020-06-19 23:59 (CEST)

A-1104

Your abstract is complete (not submitted).